

Conduction-band states and surface core excitons in InSb(110) and other III-V compounds

Jürgen Faul, Georg Neuhold,* and Lothar Ley

Institut für Technische Physik, Friedrich-Alexander-Universität Erlangen-Nürnberg, D-91058 Erlangen, Germany

Jordi Fraxedas

European Organization for Nuclear Research (CERN), CH-1211 Genf 23, Switzerland

Stefan Zollner

Ames Laboratory and Department of Physics and Astronomy, Iowa State University, Ames, Iowa 50011

John D. Riley and Robert C. G. Leckey

Department of Physics, La Trobe University, Bundoora, Victoria, 3083 Australia

(Received 19 January 1994; revised manuscript received 20 May 1994)

Angle-resolved constant-initial-state spectroscopy from the valence-band maximum (VBM) as the initial state was used to determine the conduction-band energies at the Γ point up to 30 eV above the VBM for InSb. Structure in the spectra up to 20 eV could be assigned to particular interband transitions by comparison with empirical pseudopotential calculations. Autoionizing resonances due to surface core excitons have been observed. From their energies a surface-core-exciton binding energy of 0.5 eV for InSb has been determined. Both results are discussed in light of our previous work on the conduction-band states and surface core excitons of several III-V semiconductors.

I. INTRODUCTION

The experimental determination of the valence-band structure of semiconductors by means of angle-resolved photoemission spectroscopy (ARPES) relies on certain assumptions about the energy dispersion of the final states involved in the transitions. These assumptions are necessary to determine the wave vector \mathbf{k} of the initial states because its component perpendicular to the surface, k_{\perp} , is not conserved in the photoemission process. To this end the free-electron parabolic (FEP) is widely used as a model dispersion for the conduction-band states¹ which provides the necessary link between final-state energy and k_{\perp} . A question of importance is thus whether this model can be justified by experimental results.

In earlier publications we have used angle-resolved constant-initial-state (ARCIS) experiments to determine the conduction-band states in GaAs, InP, InAs, GaSb, and GaP(110) at Γ , the Brillouin-zone center, up to an energy of 66 eV above the valence-band maximum (VBM).^{2,3} Here, we report on an extension of these investigations to InSb. Furthermore, it complements an earlier \mathbf{k} -resolved inverse photoemission investigation which yields conduction-band states up to about 5 eV above VBM.⁴

ARCIS is a variant of photoemission spectroscopy.⁵ Thereby it is ensured that photoemission always proceeds from initial states with the same energy E_i . Because for InSb the VBM lies at $\mathbf{k}=0$ (Γ -point) direct transitions connect this initial state E_i to final states at Γ only. While no previous ARCIS study on InSb(110) has been carried out until now, there are several investigations of the valence-band structure of InSb(110) by ARPES dedi-

cated to both the surface state^{6,7} and the bulk state dispersion.^{8,9}

II. RESULTS AND DISCUSSION

The measurements were performed with synchrotron radiation at the Berliner Elektronen-speicherring-Gesellschaft für Synchrotronstrahlung (BESSY). Experimental details like setup, sample preparation by cleaving *in situ*, and peak detection are described elsewhere.² All spectra presented here were excited with *p*-polarized light impinging under 45° with respect to the surface normal along the $[1\bar{1}1]$ azimuth onto the sample.

For a model independent determination of Γ -point conduction-band state energies the judicious choice of the initial-state energy is important because only at the VBM as initial state the \mathbf{k} vector of the initial and thus also of the final states is unambiguously known, namely, $\mathbf{k}=0$. For this reason particular attention has to be paid to occupied surface states near the VBM which could mask the onset of emission from the top of the valence bands.

There are three investigations of the top most surface state on the (110) surface of InSb. Two of them were dedicated to the dispersion around the \bar{X} point⁶ and the \bar{M} point⁷ only whereas the authors of the third study were able to follow the dispersion of the surface state over the whole surface Brillouin zone.¹⁰ They observed a decreasing intensity of this state when approaching the $\bar{\Gamma}$ point. Because of the weakness of this surface state near $\bar{\Gamma}$ we employed for the determination of the VBM the procedure described previously.²

Figure 1 shows a normal-emission constant initial-state spectrum of InSb. During the recording of the ARCIS spectra the photoemission current from the last focusing

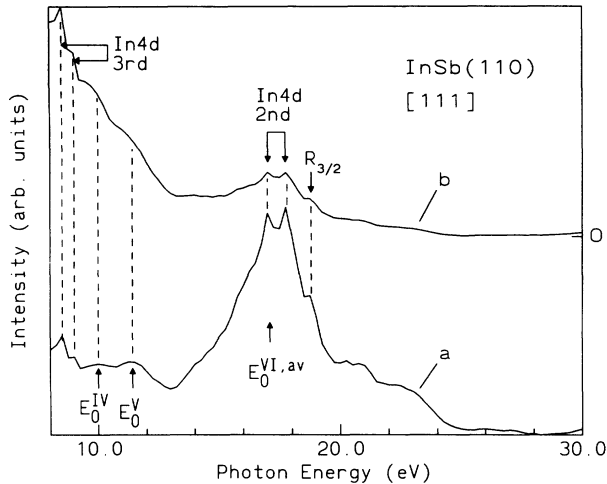


FIG. 1. Normal-emission ARCIS spectra for InSb in the energy range between 8 and 30 eV. The bottom curve (a) displays the original data while the top spectrum (b) is normalized to the mirror current. Second- and third-order light contributions are labeled as “2nd” and “3rd” respectively.

mirror in the beamline was monitored. This current is under certain assumptions proportional to the photon flux leaving the monochromator.² Thus, the curve labeled *a* in Fig. 1 shows the raw ARCIS data and curve *b* displays this spectrum normalized to the mirror current. The labels “ E_0^i ” denote interband transitions that will be discussed later.

The feature labeled $R_{3/2}$ in Fig. 1 is due to a surface-core-exciton resonance involving the In $4d_{3/2}$ core level where oscillator strength is transferred from a surface core exciton to a valence electron. The $4d_{5/2}$ part of the resonance is hidden under direct emission from the In $4d$ states, excited with second-order light of the monochromator, and a group of interband transitions labeled $E_0^{VI,av}$ (see below). To identify the core-exciton resonance clearly the initial-state energy was shifted from the VBM to 0.8 eV below VBM as shown in Fig. 2 (upper curve). For this choice of initial-state energy the second-order In $4d$ emission is shifted by 0.8 eV and the interband transitions are spread over a wider energy range due to the higher volume in \mathbf{k} space that is available when the initial-state energy is moved away from VBM.

Because the resonant enhancement applies to all valence states¹¹ the surface-core-exciton resonance is evident in both ARCIS spectra of Fig. 2. There we determine the resonance energies as 17.8 ± 0.1 eV and 18.7 ± 0.1 eV for excitation from the In $4d_{5/2}$ and $4d_{3/2}$ core level, respectively. This is in good agreement with previously published partial-yield data¹² where a resonance energy of 17.75 eV was obtained for the In $4d_{5/2}$ component. From the spectrum taken with the VBM as initial state the core-level binding energy results as 17.0 and 17.8 eV for the $4d_{5/2}$ and the $4d_{3/2}$ component, respectively.

To estimate the exciton binding energy E_{EXC} it is necessary to know the minimum energy of the empty surface-state band. As far as we know there is only one investigation of the surface conduction-band structure of InSb(110) published in the literature.⁴ There, an empty

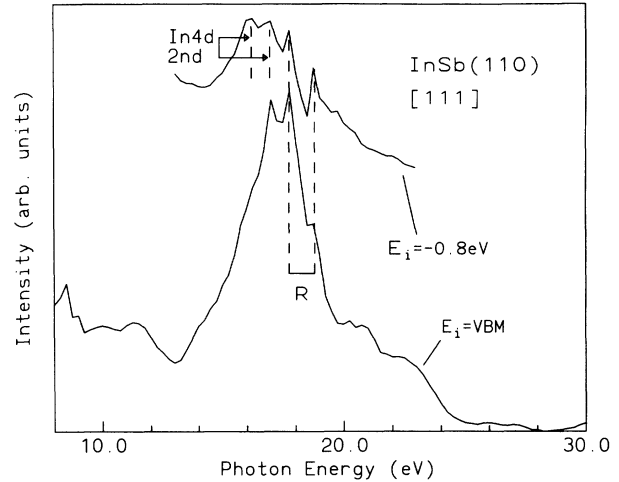


FIG. 2. Normal-emission ARCIS spectra for InSb in the energy range between 8 and 30 eV. The bottom curve shows the spectrum with the VBM as initial states while the initial-state energy of the upper curve is chosen to lie 0.8 eV below the VBM. Label “R” indicates surface-core-exciton resonances and second-order light contributions are labeled as “2nd.”

surface state for $\mathbf{k}=0$ ($\bar{\Gamma}$ point) was reported at 1.9 eV above the VBM. However, due to the “*p*”-like character of the lowest surface conduction band we assume its minimum to lie not at $\bar{\Gamma}$ but at \bar{X} like the surface band minima of GaP, GaAs, and GaSb (110).^{10,13}

The energy of the unoccupied surface state at \bar{X} is obtained by combining the value for the surface electronic gap of 2.1 eV (Ref. 14) with the value for the occupied surface state of 1.0 eV below the VBM both measured at the \bar{X} point in the surface Brillouin zone.⁶ This yields an energy of 1.1 eV above VBM for the empty surface state at \bar{X} in InSb. Taking in addition the surface core-level shift of 0.2 eV towards higher binding energies between the bulk and the surface core level into account¹⁵ we arrive at an exciton binding energy of 0.5 ± 0.2 eV for the In $4d_{5/2}$ core level exciton in InSb.

In Fig. 3 we compare this result with exciton binding energies obtained previously for other III-V semiconductors.^{2,3} There, the bulk conduction-band minimum E_{CBM} , the unoccupied surface-state energy E_{SS} , and the excitonic energy E_{EXC} are displayed with respect to the VBM. The arrows indicate the corresponding surface-core-exciton binding energies. The materials are ordered, separated into In and Ga compounds, according to the lattice constants which are listed at the bottom of the figure.

The core exciton binding energies span a range of 0.3–1.5 eV and are thus appreciably larger than those of the better known band to band excitons. Reasons for this increase are already given in our previous paper.² Del Sole showed¹⁶ that surface core excitons in GaAs are well described in the effective-mass approximation with central cell corrections contributing a mere 25% to the binding energy. Aside from this correction the decisive factor determining E_{EXC} is the surface Rydberg $R = \mu \epsilon^4 / 8h^2 (\epsilon_0 \epsilon_{surf})^2$ with an effective mass μ that is

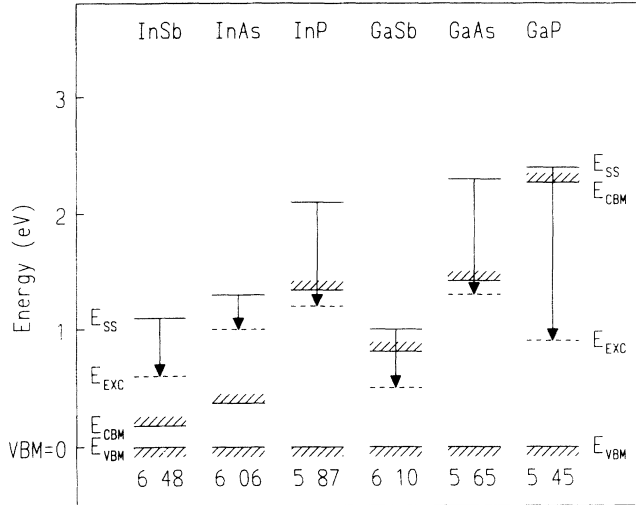


FIG. 3. Comparison of the exciton binding energy E_{EXC} , the unoccupied surface-state energy E_{SS} , the conduction-band minimum E_{CBM} , and the surface-core-exciton binding energy marked as arrows for six different III-V semiconductors. On the bottom of the viewgraph the lattice constants are quoted.

equal to the effective electron mass of the empty surface state because the hole mass can be considered infinite for a core level. $\epsilon_{\text{surf}} = (\epsilon_{\infty} + 1)/2$ is the surface dielectric constant, i.e., the average of the electronic bulk (ϵ_{∞}) and vacuum (1) dielectric constant. If the central-cell corrections do not vary too much from compound to compound and the del Sole ansatz is correct we expect E_{EXC} to vary like R and $E_{\text{EXC}}\epsilon_{\text{surf}}^2/\mu$ should be constant where we have discarded the constant ϵ_0 .

In lieu of exact values for the effective electron mass we approximate the surface conduction-band dispersion by $E(k) = (\Delta E_{\text{SS}}/2)\cos[2\pi k/g]$ with the reciprocal surface lattice vector g along the $(\bar{\Gamma})-(\bar{X})$ direction and the surface bandwidth $\Delta E_{\text{SS}} = E(\bar{\Gamma}) - E(\bar{X})$. Thus, the effective electron mass as the reciprocal band curvature at \bar{X} is $\mu = \hbar^2 / [\partial^2 E(k)/\partial k^2] = \hbar^2 g^2 / (2\pi^2 \Delta E_{\text{SS}})$.

Table I summarizes the exciton binding energies for all six materials. Also included are values for the surface dielectric constants $\epsilon_{\text{surf}} = (\epsilon_{\infty} + 1)/2$ where the electronic parts of the bulk dielectric constants ϵ_{∞} were taken from Ref. 17. The effective masses μ in Table I are determined as described above from experimentally determined bandwidths.^{10,13} Because for InAs and InP position and

dispersion of the surface states are not known this quantity is only listed for InSb and the three Ga compounds.

In the last column of this table we list $E_{\text{EXC}}\epsilon_{\text{surf}}^2/\mu$ which is expected to remain constant in the effective-mass approximation for the different materials by neglecting possible changes in the 2D confinement of the exciton and the central-cell corrections. This expectation is only partially borne out by the results. We do note, however, that $E_{\text{EXC}}\epsilon_{\text{surf}}^2/\mu$ varies by only 29% for the Ga compounds whereas the corresponding exciton binding energies vary by a factor of three. Thus, the surface Rydberg appears to be indeed responsible for most of the variation in E_{EXC} with the remaining differences due to the corrections alluded to above.

For the discussion of the band transitions we now return to the spectra of Fig. 1. All structures not yet identified as higher-order core-level emission or resonances are possible candidates for interband transitions at the center of the Brillouin zone. To exclude monochromator artefacts resulting in structure in the raw data we also present normalized data in Fig. 1 as mentioned earlier.

The assignment of the spectral features to particular band transitions was achieved by comparison with empirical pseudopotential calculations. They were performed by using 113 plane waves in a Cohen-Bergstresser scheme with the form factors determined by Cohen and Bergstresser¹⁸ resulting in energy eigenvalues for the conduction-band Γ points of 0.54, 4.0, 6.9, 7.3, 10.6, 11.9, 21.1, 21.2, 21.4, and 21.7 eV. The labeling of the transitions follows the one introduced in the optical literature where E_0 stands for the fundamental gap at Γ and higher transitions are labeled $E_0^{\text{I}}, E_0^{\text{II}}, \dots$

In this way we identify the structure at 10.0 eV with E_0^{IV} , at 11.4 eV with E_0^{V} , and the one at 17.1 eV with $E_0^{\text{VI,av}}$. The latter one is superimposed on the In 4d core line emission excited with second-order light. Because of this we are in no position to attribute individual transitions to particular conduction-band states and therefore $E_0^{\text{VI,av}}$ refers to the center of gravity of a number of closely spaced transitions around 17 eV. Already known for InSb are E_0 at 0.235 eV and E_0^{I} at 4.2 eV as obtained by optical experiments.¹⁹

By closer inspection of Fig. 1 it is obvious, that the $E_0^{\text{VI,av}}$ transition is the most intense one. As shown earlier³ this transition is associated with final states derived from the (220) umklapp of the free-electron parabola.

TABLE I. Exciton binding energies E_{EXC} as determined by our work. Also included in this table are values for the surface dielectric constant $\epsilon_{\text{surf}} = (\epsilon_{\infty} + 1)/2$, the surface g vector along $(\bar{\Gamma})-(\bar{X})$, the surface bandwidth ΔE_{SS} , and the effective mass $M\mu$. $E_{\text{EXC}}\epsilon_{\text{surf}}^2/\mu$ is explained in the text.

	E_{EXC} (eV)	ϵ_{surf}	g (\AA^{-1})	ΔE_{SS} (eV)	μ/m_0	$E_{\text{EXC}}\epsilon_{\text{surf}}^2/\mu$ (eV)
InSb	0.5±0.2	8.3	2.74	0.8	1.81	19.0
InAs	0.3±0.2	6.6	2.93			
InP	0.9±0.2	5.3	3.03			
GaSb	0.5±0.2	7.7	2.91	0.9	1.82	16.2
GaAs	1.0±0.2	6.0	3.15	0.7	2.73	13.2
GaP	1.5±0.2	5.1	3.26	0.6	3.42	11.5

Transitions into the (220) branch of the FEP couple particular well to the outgoing electron wave along the normal [110] direction ("primary cone emission").²⁰

In lieu of other data on final-state positions in this energy range we compare the results for InSb with our previous data for GaSb, InAs, InP, GaAs, and GaP.^{2,3} This is done in Fig. 4 where all the band transitions are plotted versus G_{220} , the smallest reciprocal-lattice vector in the [110] direction. On top of Fig. 4 the different materials are denoted. The dashed parabolic lines indicate the position of the (111), (200), and (220) umklapps of the FEP at Γ , respectively. For its calculation we used an average inner potential of 9.0 eV. Here, only bulk umklapp vectors have been considered because surface umklapps which are thus disregarded are very weak in intensity.³

In our previous work we associated particular band transitions E_0^i to specific FEP umklapp vectors at Γ .³ Thus, crosses in Fig. 4 indicate transitions that are derived from the (111) umklapp, diamonds from the (200) umklapp, and squares from the (220) umklapp, respectively. Transition energies above 8.5 eV are determined by ARCIS while the lower energy data stem from optical and inverse photoemission experiments.¹⁹ The individual transitions are labeled for GaP on the left-hand side of the figure. Only for GaP and GaAs have all transitions been identified. For InSb and InAs transitions E_0^{II} and E_0^{III} , for GaSb E_0^{III} , and for InP E_0^{III} and E_0^{IV} are missing.

It is expected that by turning on the crystal potential the degeneracy of the free-electron states is lifted. The center of gravity of the transitions, however, is supposed to be unchanged as long as interactions with states further away in energy are neglected. This behavior is clearly reproduced by transitions derived from the (111) umklapp (indicated by crosses). The situation for the (200)

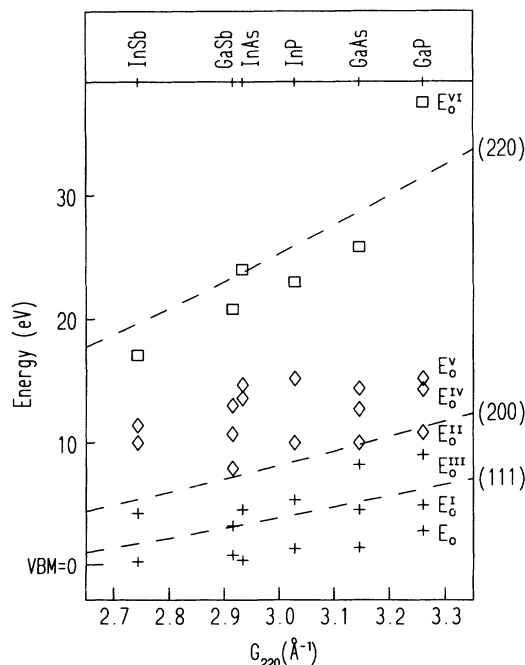


FIG. 4. Comparison of interband transition energies for the different materials. The energies are plotted versus the length of the reciprocal-lattice vector G_{220} . The meaning of the different symbols is explained in the text.

umklapp, however, is different. The center of gravity of the transitions derived from this umklapp seems to be shifted to higher energies after turning on the crystal potential for all materials which suggests stronger mixing of these states with lower lying than with higher lying states.

For transitions derived from the (220) umklapp the symbols mark the center of gravity position of a group of transitions in the experimental data. This center strongly depends on the transition probability of each single transition contributing to the experimental feature in the ARCIS spectrum. Small changes in cross section may therefore affect the center of gravity. Due to this fact a direct comparison of $E_0^{\text{VI,av}}$ with the (220) umklapp is less meaningful than in the other cases.

In addition, for the calculation of the FEP energies in Fig. 4 the same inner potential of 9.0 eV was used for all the materials. For InSb, for example, Middelmann *et al.* determined an inner potential of 7.0 eV.⁸ However, the choice of 7.0 eV for the inner potential results in an upward shift by 2 eV for the free-electron energies which worsens the agreement with $E_0^{\text{VI,av}}$ for InSb.

As demonstrated earlier transition peaks at energies above $E_0^{\text{VI,av}}$ are supposed to be very weak according to our transition probability calculations.² This was borne out by the spectra above 30 eV which were dominated by the Sb 4d core-level emission excited with second-order light.

III. CONCLUSION

Angle-resolved constant initial-state (ARCIS) spectra have been performed to study conduction-band critical points at the center of the Brillouin zone up to 30 eV above VBM in InSb. Experimental features below 20 eV have been identified with direct interband transitions on the basis of EPM calculations. The data were also compared with our previous measurements on a variety of III-V semiconductors. All the systems exhibit similar transitions. However, a systematic trend of transition energies with the latter constants expected on the basis of the free-electron model could only be established in the most general sense.

An autoionization resonance involving a surface core exciton was observed for InSb. The binding energy of this core exciton, E_{EXC} , was determined and compared with that of other III-V semiconductors. For the Ga compounds at least, an effective-mass approach to the exciton binding energy as suggested by del Sole accounts for most of the observed variations in E_{EXC} .

ACKNOWLEDGMENTS

This work was supported by the Bundesministerium für Forschung und Technologie, Contract No. 05 5 WEDA B 3, and by the Australian Research Council. The authors would like to thank the staff of BESSY, especially W. Braun, for their help and hospitality during the experiments. We also acknowledge the assistance of R. Denecke, T. Seyller, R. Eckstein, and J. Con Foo during the experiments.

*Present address: Fritz-Haber-Institut, Faradayweg 4-6, D-14195 Berlin, Germany.

- ¹R. C. G. Leckey and J. D. Riley, *Crit. Rev. Solid State Mater. Sci.* **17**, 307 (1992).
- ²J. Faul, G. Neuhold, L. Ley, J. Fraxedas, S. Zollner, J. D. Riley, and R. C. G. Leckey, *Phys. Rev. B* **47**, 12 625 (1993).
- ³J. Faul, G. Neuhold, L. Ley, J. Fraxedas, S. Zollner, J. D. Riley, and R. C. G. Leckey, *Phys. Rev. B* **48**, 14 301 (1993).
- ⁴W. Durbe, D. Straub, and F. J. Himpsel, *Phys. Rev. B* **35**, 5563 (1987).
- ⁵J. A. Knapp and G. J. Lapeyre, *Il Nuovo Cimento B* **39**, 693 (1977).
- ⁶H. Höchst and I. Hernandez-Calderon, *Phys. Rev. B* **30**, 4528 (1984).
- ⁷H. W. Richter, J. Barth, J. Ghijsen, R. L. Johnson, and L. Ley, *J. Vac. Sci. Technol. B* **4**, 900 (1986).
- ⁸H. U. Middelman, L. Sorba, V. Hinkel, and K. Horn, *Phys. Rev. B* **34**, 957 (1986).
- ⁹G. P. Williams, F. Cerrina, G. J. Lapeyre, J. R. Anderson, R. J. Smith, and J. Hermanson, *Phys. Rev. B* **34**, 5548 (1986).
- ¹⁰R. Manzke and M. Skibowski, *Phys. Scr.* **T31**, 87 (1990).
- ¹¹C. Janowitz, R. Manzke, M. Skibowski, Y. Takeda, Y. Miyamoto, and K. Cho, *Surf. Sci. Lett.* **275**, L669 (1992).
- ¹²D. E. Eastman and J. L. Freeouf, *Phys. Rev. Lett.* **34**, 1624 (1975).
- ¹³P. Perfetti and B. Reihl, *Phys. Scr.* **T25**, 173 (1989).
- ¹⁴H. Carstensen, R. Claessen, R. Manzke, and M. Skibowski, *Phys. Rev. B* **41**, 9880 (1990).
- ¹⁵V. Hinkel, L. Sorba, and K. Horn, *Surf. Sci.* **194**, 597 (1988).
- ¹⁶R. Del Sole and E. Tosatti, *Solid State Commun.* **22**, 307 (1977); *Nuovo Cimento B* **39**, 791 (1977).
- ¹⁷W. Mönch, *Semiconductor Surfaces and Interfaces* (Springer-Verlag, Berlin, 1993), p. 331.
- ¹⁸M. L. Cohen and T. K. Bergstresser, *Phys. Rev.* **141**, 789 (1966).
- ¹⁹Landolt-Börnstein, *Numerical Data and Functional Relationships in Science and Technology, New Series III*, Vol. 22a (Springer-Verlag, Berlin, 1989), and references therein; Landolt-Börnstein, *Numerical Data and Functional Relationships in Science and Technology, New Series III*, Vol. 23a (Springer-Verlag, Berlin, 1989), and references therein.
- ²⁰G. D. Mahan, *Phys. Rev. B* **2**, 4334 (1970).